Collagenase Nanoparticles Enhance the Penetration of Drugs into Pancreatic Tumors

Assaf Zinger[1,8], Lilach Koren[1,8], Omer Adir[1], Maria Poley[1], Mohammed Alyan[1], Zvi Yaari[1], Nadav Noor[6], Nitzan Krinsky[1], Assaf Simon[1], Hadas Gibori[2], Majd Krayem[1], Yelena Mumblat[1], Shira Kasten[1], Sivan Ofir[1], Eran Fridman[3], Neta Milman[3], Michael M. Lübtow [4], Lior Liba[5], Jeny Shklover[1], Janna Shainsky-Roitman[1], Yoav Binenbaum[3], Dov Hershkovitz[7], Ziv Gil[3], Tal Dvir[6], Robert Luxenhofer[4], Ronit Satchi-Fainaro[2] and Avi Schroeder[1,*]

[1]Laboratory for Targeted Drug Delivery and Personalized Medicine Technologies, Department of Chemical Engineering, Technion – Israel Institute of Technology, Haifa 3200003, Israel
[2]Department of Physiology and Pharmacology, Sackler Faculty of Medicine, Tel Aviv University, Tel Aviv 6997800, Israel
[3]Department of Otolaryngology Head and Neck Surgery, Rambam Healthcare Campus, Technion-Israel Institute of Technology, Haifa 3200000, Israel
[4]Functional Polymer Materials, Lehrstuhl für Chemische Technologie der Materialsynthese, Julius-Maximilians-Universität Würzburg, Röntgenring 11, Würzburg 97070, Germany
[5]The Ruth and Bruce Rappaport Faculty of Medicine, Technion – Israel Institute of Technology, Haifa 3200003, Israel
[6]The School for Molecular Cell Biology and Biotechnology and the Department of Materials Science and Engineering, Tel Aviv University, Tel Aviv 6997800, Israel.
[7]Department of Pathology, Tel-Aviv Sourasky Medical Center, Sackler Faculty of Medicine, Tel-Aviv University, Tel Aviv 6997800, Israel
[8]These authors contributed equally to this work

*Corresponding author E-mail: (AS) avids@technion.ac.il

Abstract

Overexpressed extracellular matrix (ECM) in pancreatic ductal adenocarcinoma (PDAC) limits drug penetration into the tumor and is associated with poor prognosis. Here, we demonstrate that a pretreatment based on a proteolytic-enzyme nanoparticle system, disassembles the dense PDAC collagen stroma, and increases drug penetration into the pancreatic tumor. More specifically, the collagozome, a 100-nm liposome encapsulating collagenase, was rationally designed to protect the collagenase from premature deactivation and prolonged its release rate at the target site.

Collagen is the main component of the PDAC stroma, reaching 12.8±2.3%vol in diseased mice pancreases, compared to 1.4±0.4% in healthy mice. Upon intravenous injection of the collagozome, ~1% of the injected dose reached the pancreas over 8 hours, reducing the level of fibrotic tissue to 5.6±0.8%.

The collagozome pretreatment allowed increased drug penetration into the pancreas and improved PDAC treatment. PDAC tumors, pretreated with the collagozome followed by paclitaxel micelles, were 87% smaller than tumors pretreated with empty liposomes followed by paclitaxel micelles. Interestingly, degrading the ECM did not increase the number of circulating tumor cells or metastasis. This strategy holds promise for degrading the extracellular stroma in other diseases as well, such as liver fibrosis, enhancing tissue permeability before drug administration.

Keywords: pancreatic cancer, nanoparticle, extracellular matrix, fibrosis, collagen, liposome, paclitaxel micelles.

With less than 8% five-year survival rate, pancreatic ductal adenocarcinoma (PDAC) remains one of the deadliest cancers with insufficient treatment modalities. One primary reason for this poor prognosis is the excess growth of a fibrotic extracellular matrix (ECM) stroma around the cancerous cells, limiting the penetration of drugs and immune cells into the tumor.[1,2]

Collagen, a triple-helix protein, is the main structural component in the PDAC-ECM.[3] Collagen viscoelastic properties play a major role in constructing healthy tissues, but pathologic excess production of collagen can contribute to chemoresistance.[4]

The ECM stroma of pancreatic tumors generates high interstitial fluid pressures that results in vascular collapse, further limiting drug uptake from circulation.[5,6] Recent studies have suggested that manipulating the ECM can decrease tumors' drug resistance and improve the outcome of chemotherapy treatments in pancreatic cancer.[7-9] For example, inhibiting Hedgehog signaling pathways, which are associated with ECM construction, increased the penetration of chemotherapy into the tumor.[1,10] In another study, a combination therapy of the anti-fibrotic agent pirfenidone with chemotherapy, also suppressed tumor growth by reducing collagen synthesis through pancreatic stellate cell regulation.[10]

Another abundant component of the ECM is hyaluronic acid (HA). HA can be rapidly turned over by hyaluronidase. Ongoing Phase III Clinical trials of a combined therapy of PEGylated recombinant human hyaluronidase with gemcitabine for PDAC treatment have shown to prolong PDAC survival.[11]

Collagenase type-I (Enzyme Commission (EC) number 3.4.24.3) is a water-soluble matrix metalloprotease with specificity towards collagen fibers.[12,13] Once activated by its natural co-factors, Ca^{+2} and Zn^{+2}, the half-life of collagenase varies from tissue to tissue, declining to single minutes when injected into systemic circulation.[14] Thereby, most therapeutic applications will require a formulation to protect the enzyme from early deactivation before reaching the target site.[15,16]

Nanotechnologies are emerging therapeutic tools with promise to target diseased tissues accurately.[17-19] Abraxane, a FDA-approved paclitaxel-loaded 110-nm particle, is used for treating PDAC patients in combination with gemcitabine.[20] Gold nanoparticles,[21] polymeric micelles[22-25] and liposomes[26,27] have also been demonstrated as nanoscale drug delivery systems for treating PDAC.

Liposomes are commonly used clinical nanoparticles, composed of a lipid bilayer that surrounds an inner aqueous core.[28] Accordingly, hydrophobic drugs can be encapsulated in the liposome membrane and hydrophilic drugs can be loaded into the inner aqueous core.[29]

In this study we developed a nanoscale liposomal drug delivery system that encapsulates collagenase type-I and releases it in the tumor microenvironment. The released enzyme disassembles the collagen component of the PDAC-ECM, leading to improved drug uptake by pancreatic tumors.

Results & Discussion

The progression of pancreatic ductal adenocarcinoma (PDAC) is accompanied by the development of a dense extracellular matrix (ECM) that acts as physical barrier, preventing from drugs to penetrate the tumor.[30-32] Collagen, a primary structural protein that is involved in healthy and pathologic tissue remodeling, is a major component of the PDAC's ECM. In this study we evaluated a nanoscale drug delivery system that targets the collagen component of the ECM, by the localized delivery of a proteolytic enzyme – collagenase type-I (Figure 1A-D). For this, we developed a nanoparticle that protected the enzyme from biodegradation and prolonged its release rate. Then, we demonstrated the natural barrier function of the PDAC-ECM. Subsequently, we show that collagenase nanoparticles (collagozome's), successfully degrade collagen in PDAC tumors and in fibrotic livers. Finally, we measured the therapeutic efficacy of pretreating the tumor with collagozome followed by a drug.

Collagenase nanoparticles (collagozome). Encapsulating proteins in nanoparticles must overcome several challenges, including possible denaturing of the protein during the loading process and maintaining a therapeutic release rate at the target site. Because the half-life of collagenase in circulation is extremely short, we loaded collagenase into liposomes (i.e., the collagozome), which protected it from early deactivation in the plasma and prolonged the enzyme' activity (Figure 1E). The primary phospholipid used to construct the liposomes was 1,2-dimyristoyl-sn-glycero-3-phosphocholine (DMPC), comprised of two 14:0 hydrocarbon chains conjugated to the phosphocholine head

group. DMPC's phase transition temperature (T_m) is 24-25.5 °C , which is favorable for loading collagenase without compromising the enzyme's activity during the encapsulation process.[33,34] To modulate the collagenase release kinetics from the collagozome we varied the cholesterol content in the phospholipid bilayer.[35] Specifically, we tested the effect three different cholesterol concentrations (0, 15 and 39 mole%) have on the release kinetics. Collagozomes having 39 mole% cholesterol, demonstrated a prolonged enzyme release profile compared to the other formulations (Figure 1F) – less than 40% of the encapsulated collagenase was released over 24 hours. No significant difference in the enzyme release profile was observed between formulations consisting of either 0 or 15 mole% cholesterol, in which approximately 60% of the enzyme was released during 24 hours. This is explained by the effect cholesterol has on the stability of the lipid bilayer. Differential scanning calorimetry (DSC) analysis of the liposomes showed that DMPC has a sharp phase transition at 25.5°C (Figure 1G). Increasing the cholesterol content in the liposome membrane decreases the intensity of the Tm peak. At 39 mole% cholesterol no phase transition is recorded as the membrane enters a low-permeability liquid-ordered phase, explaining the prolonged release rate of the collagenase (Figure 1F).[36,37] Based on these results, we decided to proceed with our study using 100-nm collagozomes composed of DMPC enriched with 39 mole% cholesterol and DSPE-PEG, to prolong the collagozome circulation half-life (Figure 1H, Supplementary Figure S1).[38,39]

Fibrotic extracellular matrix functions as a mass transport barrier in PDAC.

We characterized the collagen content in healthy and diseased regions of the pancreas. Masson's Trichrome staining demonstrated that the collagen content in pancreatic tumors was 12.25-fold greater than the collagen content in the healthy pancreas (Figure 1I). To assess the biodistribution of nanoparticles in healthy and diseased pancreases, mice bearing PDAC were injected with 100-nm liposomes loaded with the MRI contrast agent gadolinium (Gd) and co-labeled with a fluorescent dye (rhodamine) in the lipid bilayer. Eight hours post *intravenous* administration maximal pancreatic accumulation was recorded by elemental analysis, reaching 2.65 μg-Gd/g-pancreas whereas after 14 hours the concentration decreased to 0.83 μg-Gd/g-pancreas (n=3; Figure 1J). In total, 1% of the injected dose accumulated in the pancreas. Using non-invasive *intra-vital* microscopy (Figure 1K, L) and qualitative and quantitative histological analyses (Figure 1M, N) we imaged the liposomal biodistribution within the diseased pancreas after *intravenous* injection. Interestingly, we noticed that the collagen fibrotic barrier inhibited the penetration of the liposomes into the diseased regions of the pancreas. Specifically, 97±%1 of the liposomes that reached the pancreas accumulated in the non-neoplastic regions of the pancreas (Figure $1N_{I,II}$), while the remainder accumulated in the cancerous PDAC tissue (Figure $1N_{III-V}$). Number-wise, out of approximately 1.3×10^{15} liposomes that were injected *intravenously*, only 1.3×10^{13} liposomes reached the pancreas, of which only 3.9×10^{11} liposomes reached the PDAC cancerous tissue (Supplementary Figure S1, Table S1) corresponding to 29.8 ng-Gd/g-pancreatic-tumor. MRI imaging

(9.4T) of the liposomal biodistribution confirmed that majority of the Gd was cleared by the urinary system during the first half-hour post injection (Figure 1O). However, a gradual increase in the pancreatic liposomal content was measured alongside the bladder clearance (Figure 1P). This was strengthened by ICP-OES elemental measurements done for Gd quantity in blood and urine following 30 minutes post *intravenous* injection of either free or liposomal Gd. This analysis demonstrated that majority of free Gd is secreted through the urine 30 minutes post iv injection (Figure 1Q), while liposomal Gd is mostly found circulating in blood (Figure 1R) and accumulates in tumor following 24 hours (Figure 1P). Taken together, these data emphasize the barrier the ECM poses to nanoparticle uptake into the diseased pancreas.

Enzymatic degradation of collagen in PDAC and liver fibrosis. We first sought to characterize the collagen content in healthy and diseased pancreases before and after collagenase treatment. Masson's Trichrome staining was used to quantify the collagen content in the different groups. For this characterization, pancreatic tumors were excised and incubated in collagenase solutions of different concentrations. Then, we evaluated the collagen content in three groups: healthy pancreases, pancreases with PDAC after the collagenase treatment, and, untreated pancreatic PDAC (Figure 2A, B). The effect of three collagenase concentrations (0.05, 0.1 and 0.2 mg/ml) on PDAC collagen, was compared after 8 and 24 hours (Supplementary Figure S2). The highest levels of collagen were recorded in the PDAC group=12.8±2.3% (Figure $2A_{IV}$, n=10 biological replicates) while the lowest levels were observed in the healthy pancreas 1.4±0.4%

(Figure $2A_I$, n=7 biological replicates). The level of fibrotic tissue in Masson's Trichrome staining of the pancreatic tumor in the PDAC group decreased to 1.28±0.3% (Figure$2A_{II}$) after being treated with 0.2mg/ml collagenase *ex-vivo* (n=8 biological replicates).

In-vivo, mice (n=9) bearing PDAC tumors were injected with collagozome and the collagen content of the tumor was evaluated histologically. Masson's Trichrome staining 24-hours after the treatment indicated a decreased collagen content in the tumor of 5.6±0.8% (Figure $2A_{III}$,B). Furthermore, the effect collagenase had on the microstructure of the collagen mesh *in-vivo* was also studied. Healthy pancreases, PDAC after collagenase *in-vivo* treatment and untreated PDAC were decellularized and their ECM was visualized using scanning electron microscopy (SEM, Figure 2C-E). Image analysis revealed that the collagen component in the tumor fiber mesh decreased tumor pancreatic tissue mesh density by 37% following collagozome pretreatment compared with non-treated tumor pancreatic tissue (Figure 2F). Greater openings within the mesh suggest that the collagenase treatment can enhance the uptake of drugs by reducing barriers in pancreatic tumors.

We confirmed the effect the collagozome has on degrading fibrous tissue using an additional *in vivo* biological model of liver fibrosis in mice.[40] Fibrosis is a common disorder in multiple diseases. The major cause for fibrosis is tissue injury and its abnormal repair. More specifically, persistent hepatic injury triggers chronic inflammation that is followed by worsening degrees of fibrosis and eventually cirrhosis.[41-44] Since liposomes accumulate predominantly in the liver, we examined the collagozome as a potential

treatment for liver fibrosis. Liver fibrosis was induced in mice by injecting 2ml/kg carbon tetrachloride (CCl_4) *intraperitoneally* three times a week for 2 weeks. Then, mice were treated with either empty liposomes or with collagozome (Supplementary Figure 3A). Collagen levels, indicated by Masson's Trichrome staining in the liver, were reduced by 35-49% following collagenase treatment compared to empty liposomes depending on the mode of inducing the severity of the disease (Supplementary Figure 3B, C).

We studied the effect reducing the collagen mesh density with collagenase has on the biodistribution of nanoparticles to PDAC tumors *in vivo*. Healthy and PDAC-bearing mice were treated *intravenously* with either free collagenase, empty liposomes or collagozome twice in gaps of twenty-four hours. Twenty-four hours after the second injection mice were injected with gold nanoparticles either 5, 20 or 100-nm in diameter, *intravenously*. Twenty-four hours post-injection mice were sacrificed, and organs were excised and analyzed for gold levels using ICP-OES elemental analysis (Figure 2I). The collagozome pretreatment increased the liver and pancreatic uptake of 100-nm gold nanoparticles compared to the control in PDAC baring mice (Figure 2J). Furthermore, we observed an increase in pancreatic uptake of 20-nm gold nanoparticles in healthy mice (Supplementary Figure S4B). No change was observed in 5-nm in all treatment groups. This may be explained by the ability of 5-nm particles to penetrate through the collagen mesh (Supplementary Figure S4A). No significant difference in gold nanoparticle uptake was observed in the lung, heart, kidney and blood of PDAC or healthy mice (Supplementary Figure S4, S5). Based on the superior uptake of 20- to 100-nm gold

nanoparticles after the collagozome treatment, we proceeded to test the therapeutic efficacy against PDAC using collagozome followed by a treatment of paclitaxel loaded into micelles.

Therapeutic efficacy of collagozome pretreatment followed by nanoparticulate paclitaxel on PDAC tumors, circulating cancer cells, and metastasis. To test the capacity of the collagozome to enhance drug delivery to pancreatic tumors, a two-steps approach was employed. Initially two doses of collagozome were administered in order to amplify the PDAC-collagen degradation effect. Twenty-four hours later, a dose of therapeutic paclitaxel nanoparticles was administered intravenously (Figure 3D). To evaluate the biodistribution of the therapeutic nanoparticles we loaded liposomes with two clinical contrast agents – Gd and Iodixanol. CT scans of PDAC-bearing mice after the second collagozome treatment indicated a 17% increase in uptake, compared to the control (Figure 3A). Moreover, enhanced pancreatic uptake was measured by elemental analysis of Gd (Figure 3B), specifically, 30.9 mg-Gd/g-pancreas (n=4) were measured in the collagozome treated PDAC mice, *versus* 15.1 mg-Gd/g-pancreas in mice (n=5) treated with the free enzyme (Figure 3B).

To test the therapeutic efficacy, mice bearing orthotopic PDAC tumors (mCherry-labeled KPC cell line) were pretreated twice with the collagozome and 24-hr later were administered 30-nm micelles loaded with paclitaxel (10mg/kg-body-weight) (Figure 3D).[45] Five days after the paclitaxel treatment, the tumors sizes were scanned using a whole-animal imaging system (IVIS). The average normalized tumor radiance *decreased*

by 62±8.3% in the collagozome-pretreated group (n=5), while the tumor radiance *increased* by 16% in the control group treated with paclitaxel micelles without the collagozome pretreatment (n=5, Figure 3D, E, F). Administering three cycles of collagozome pretreatments followed by micellar paclitaxel (Figure 3G), achieved an even better therapeutic outcome. Micro-ultrasound measurements demonstrated the pancreatic tumor size *decreased* by 87% when paclitaxel micelles were combined with the collagozome pretreatments, compared to mice pretreated with empty liposomes plus paclitaxel micelles, or by 60% using a free collagenase pretreatment plus the paclitaxel micelles (Figure 3H, Supplementary Figure S6). Comparing the effect of free collagenase or of the collagozome, without a drug, had similar effect on the tumor (Figure 3I). Masson's Trichrome histological staining showed that collagen levels within tumors were reduced by 43% in mice pretreated with collagozome compared to empty liposomes, and by 31% in mice pretreated with free collagenase (Figure 4A-D). A reduction in collagen 3 alpha (col3a) and smooth muscle actin (SMA) mRNA expression levels was also observed in collagozome treated PDAC tumors (Figure 2G, H). Based on these findings, we conclude that pretreating the PDAC tumor with the collagozome improves the therapeutic outcome.

Delivering collagenase has the potential to act as a double-edged sword, by harming healthy organs or altering the tumor extracellular matrix in a manner that releases cancerous cells from the primary tumor into circulation.[46,47] Therefore, we quantified the circulating tumor cells (CTCs) in mice treated with collagozome and the untreated control. No significant difference in the CTC blood count was observed among more than 300,000

cells that were analyzed in either group after twenty-four hours (Figure 4E; n=4). Furthermore, metastatic cells were not detected in the liver,[48] brain, spleen and lungs seven days after either the collagozome treatment or in the combined collagozome and paclitaxel treatment (Figure 4F). These data suggest that the collagozome degrades the dense tumor ECM allowing nanomedicine penetration, but in a manner that is insufficient to release cancer cells into systemic circulation.[48,49]

To test the safety of the collagozome treatment, we sacrificed healthy mice twenty-four hours after *intravenous* injections of collagozome. Hematoxylin and eosin (H&E) and Masson's Trichrome staining of the liver, spleen, kidneys and lungs did not indicate any major physiological damage after collagozome treatments (Figure 4G). To evaluate the effect of collagozome on organ function we collected blood from the control and test groups (n=4 biological replicates). Several differences were noticed when comparing blood gases and the chemistry blood panel in the collagozome-treated and untreated mice (Figure 4H, I). Specifically, alanine transaminase (ALT) was higher in the untreated group, and amylase (AMY) was higher in the collagozome group (Figure 4I). In a complete red blood cell analysis, somewhat higher levels of hemoglobin (HGB) and lymphocytes (%LYM) were observed among the control group, while higher levels of eosinophils (%EOS) were observed among the test group, however, all fall within normal blood ranges (n=4 biological replicates, Figure 4J).

Conclusions

A major factor affecting survival rates in PDAC patients is the inability to completely resect the tumor.[50,51] Neoadjuvant and next-generation therapies, including immunotherapy and gene therapy, can turn the course of this disease.[20, 52-54] However, to be effective, medicines must be able to penetrate the dense stroma of the diseased pancreas.[5] In this study we remodeled the tumor ECM using collagenase loaded into liposomes (collagozome) that digested the collagen component of the pancreatic tumor stroma. We found that controlled delivery of a proteolytic enzyme can improve tumor treatment, with minimal harm to healthy organs. The collagozome nanoparticle protected the collagenase enzyme from early deactivation in the plasma and modulated the enzyme release profile inside the tumor. The nanoparticulate enzyme was more effective than the free enzyme in degrading the tumor ECM and facilitating enhanced drug uptake. Excess collagen synthesis is a common pathology in many life-threatening diseases.[55-59] We demonstrate here that proteolytic collagenase nanoparticles can target this pathologic extracellular tissue. In the future, such pretreatments may become standard of care for conditioning the diseased site before administering a medicine.

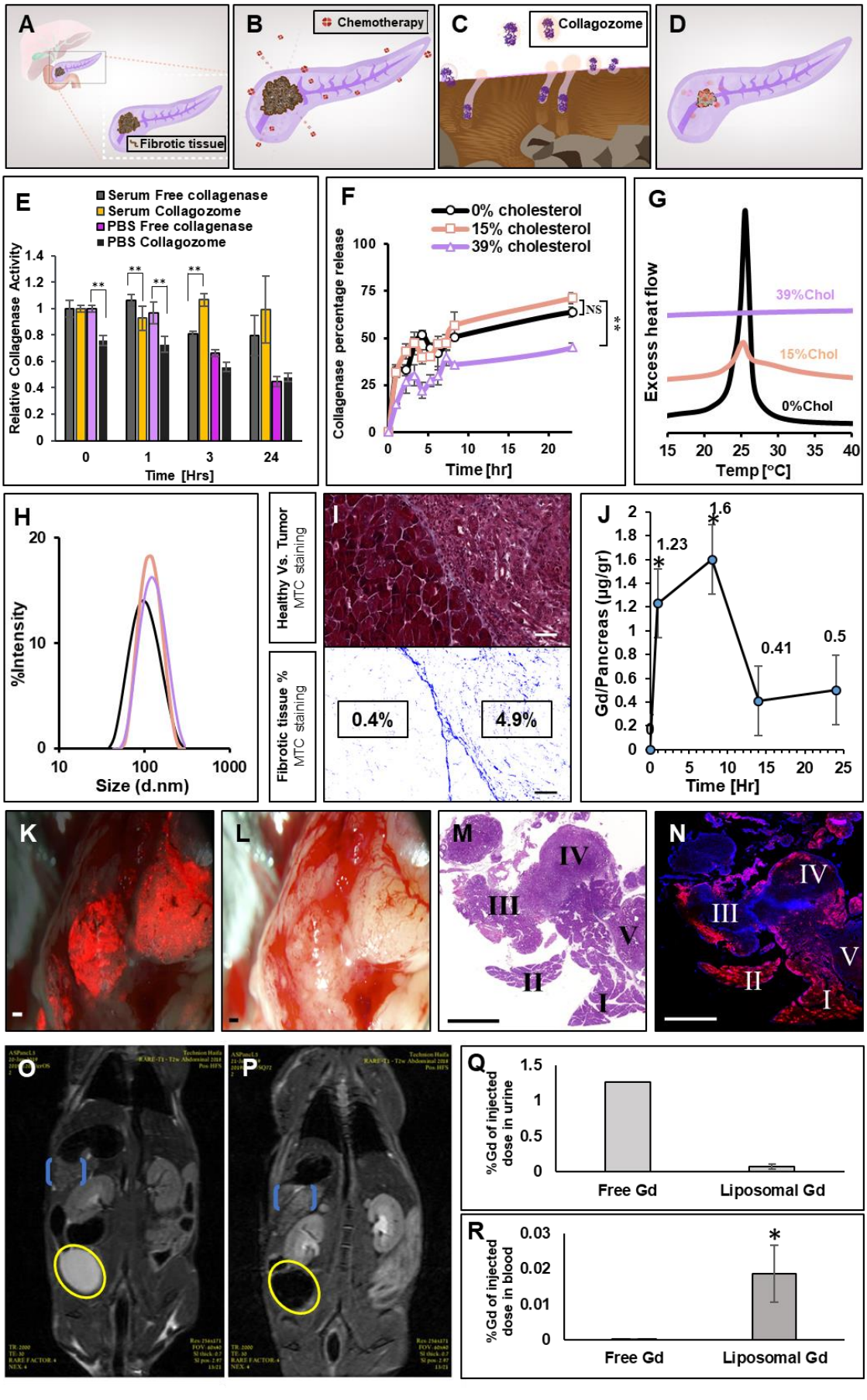
A
Fibrotic tissue
B
Chemotherapy
C
Collagozome
D
E
Serum Free collagenase
Serum Collagozome
PBS Free collagenase
PBS Collagozome
Relative Collagenase Activity
Time [Hrs]
F
0% cholesterol
15% cholesterol
39% cholesterol
Collagenase percentage release
Time [hr]
NS
G
39%Chol
15%Chol
0%Chol
Excess heat flow
Temp [°C]
H
%Intensity
Size (d.nm)
Healthy Vs. Tumor MTC staining
Fibrotic tissue % MTC staining
I
0.4%
4.9%
J
Gd/Pancreas (µg/gr)
Time [Hr]
1.23
1.6
0.41
0.5
K
L
M
IV
III
V
II
I
N
IV
III
V
II
I
O
P
Q
%Gd of injected dose in urine
Free Gd
Liposomal Gd
R
%Gd of injected dose in blood
Free Gd
Liposomal Gd

<u>Figure 1</u>. Collagenase nanoparticles and biodistribution to orthotopic pancreatic PDAC tumors.

Pancreatic ductal adenocarcinoma (PDAC) is characterized by the overexpression of extracellular matrix (ECM) – schematic outline of the study (A). The dense ECM contributes to tumor drug resistance (B). Proteolytic enzymes housed within nanoparticles were used to disassemble the collagen component of the tumor ECM (C). Collagenase encapsulated liposomes, collagozome, pretreatment increased tumor' drug uptake, allowing more effective treatment (D).

Collagenase type-I encapsulation protects the enzyme from deactivation in mouse plasma. Enzyme activity was compared inside the particles and in plasma (E), (n=3) **indicates *p*-value between specified bars <0.01.

Different liposome formulations were tested to determine the optimal collagenase nanoparticle. Liposomes were composed of DMPC: cholesterol:DSPE-PEG2000; the cholesterol content in the membrane was varied (0, 15 or 39 mole%) to test the effect on prolonging the collagenase release rate at 37°C (F), (n=3) **indicates *p*-value to 39% cholesterol<0.01.

Differential scanning calorimetry (DSC) thermograms (G) and dynamic light scattering (DLS) size measurements (H) of DMPC liposomes containing 0, 15 and 39 mole% cholesterol, suspended in PBS pH 7.4. While a sharp transition temperature can be seen 25.5°C for the 0 mole% cholesterol formulation, no transition temperature is noticed in the 39 mole% formulation. Insignificant size differences were observed between the three liposome formulations.

PDAC fibrotic collagen matrix acts as a mass transport barrier. The tumor's ECM tissue has an increased collagen component (I). Collagen was stained with Masson's Trichrome in healthy and diseased pancreatic tissue. Scale bar= 50μm. **Poor nanoparticle pancreatic uptake was observed over 24 hours in PDAC-bearing mice** (J). The amount of Gd-liposomes that reached the pancreas of PDAC mice at different time intervals after an *intravenous* administration was quantified using elemental analysis (n=3) *indicates *p*-value to control <0.05.

The majority of Gd-liposomes reach the healthy region in the diseased pancreas. Fluorescent liposomes were imaged in the pancreas using *intra-vital* microscopy (fluorescent – K ,bright field – L; scale bar= 1 mm, fluorescent liposomes are labeled red). Histological H&E-staining analysis of the pancreas enabled differentiating between the healthy ($M_{I,II}$,$N_{I,II}$) and diseased segments of the pancreas (M_{III-V}, $NIII_{-V}$). Fluorescent histology of the corresponding sections (K) indicated that most of the nanoparticles are concentrated in the healthy regions of the diseased pancreas (L; Scale bar=2mm; fluorescent sections: liposomes-red, nuclei-blue, n=3).

Majority of the nanoparticles are secreted within 25 minutes after intravenous injection. Gd liposomes were injected to the tail vein and the mice were flash-scanned using 9.4Tesla MRI. The Gd signal was imaged in the bladder and

pancreas following 25 minutes (O) and 24 hours (P) tumor marked in blue, bladder marked in yellow. Gd quantity was measured *via* elemental analysis (ICP-OES) in urine (Q) and blood (R) of at least n=3 mice following 30 minutes from *intravenous* injection of either free Gd or Liposomal Gd.

All *p*-values presented were calculated according to a student's t-test with a two-tailed distribution with unequal variance. 1A-D Illustrated by Dima Zagorski.

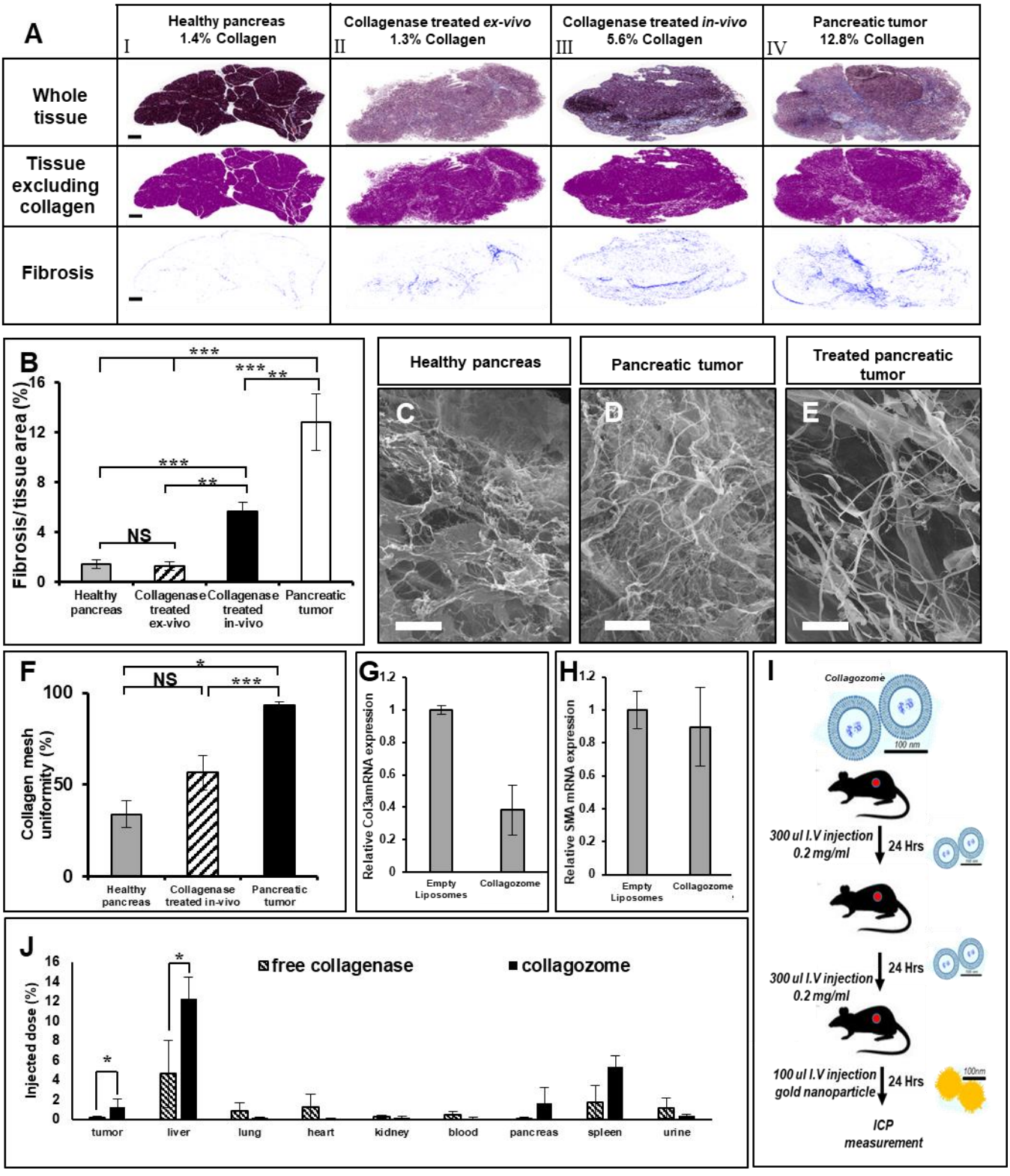
A
I Healthy pancreas 1.4% Collagen
II Collagenase treated ex-vivo 1.3% Collagen
III Collagenase treated in-vivo 5.6% Collagen
IV Pancreatic tumor 12.8% Collagen
Whole tissue
Tissue excluding collagen
Fibrosis
B
Fibrosis/tissue area (%)
Healthy pancreas
Collagenase treated ex-vivo
Collagenase treated in-vivo
Pancreatic tumor
NS
Healthy pancreas
Pancreatic tumor
Treated pancreatic tumor
C
D
E
F
Collagen mesh uniformity (%)
Healthy pancreas
Collagenase treated in-vivo
Pancreatic tumor
G
Relative Col3amRNA expression
Empty Liposomes
Collagozome
H
Relative SMA mRNA expression
Empty Liposomes
Collagozome
I
Collagozome
100 nm
300 ul I.V injection
0.2 mg/ml
24 Hrs
300 ul I.V injection
0.2 mg/ml
24 Hrs
100 ul I.V injection
gold nanoparticle
24 Hrs
100nm
ICP measurement
J
free collagenase
collagozome
Injected dose (%)
tumor
liver
lung
heart
kidney
blood
pancreas
spleen
urine

<u>Figure 2.</u> Collagenase reduces the level of fibrosis in pancreatic tumors.

Healthy pancreases (A_I), collagenase treated PDAC *ex-vivo* (A_{II}), collagenase-treated PDAC *in-vivo* (A_{III}) and non-treated PDAC (A_{IV}) collagen was stained and collagen density was evaluated (B). n=8 in each treatment group.

Collagen fibers in healthy, PDAC and collagenase-treated PDAC tumors *in-vivo* (C-E). PDAC-bearing mice and healthy mice were treated with collagozome; the pancreas was then decellularized and imaged using HR-SEM. PDAC mice after being treated with collagozome (C) and healthy pancreas (D) were compared to non-treated PDAC pancreas (E).

The collagen mesh size was measured in healthy and PDAC mice, before and after the collagenase treatment. The *in-vivo* treatment decreased the mesh size to levels found in healthy pancreas (F).

Collagen type 3 expression is reduced following collagozome pretreatment (G-H). mRNA was extracted from PDAC tumors following pretreatment with either empty or collagozome. cDNA was produced and qRTPCR was performed to determine relative expression of Collagen 3 alpha- col3a, (G) and smooth muscle actin- SMA (H). mRNA expression levels were calculated relative to GAPDH.

Biodistribution of Gold nanoparticles to various organs was enhanced in healthy and tumor-baring mice following collagenase treatment (I,J)

A schematic representation of the treatment protocol (I). Mice were administered *intravenously* with 100-nm collagozome, day after day, followed by a single dose of 100-nm gold nanoparticles (100µl, 5mg/ml) (n=5 biological replicates for each pretreatment to mice).The amount of Gold nanoparticles that reached the various organs of PDAC mice after an *intravenous* administration was quantified using elemental analysis. Results in tumor-baring mice injected with 100-nm gold nanoparticles (J).

*indicates *p*-value<0.05 according to a student's t-test with two-tailed distribution with unequal variance. **indicates *p*-value <0.01. ***indicates *p*-value<0.001 according to student's t-test with a two-tailed distribution with unequal variance.

All *P*-values presented were calculated between specified bars according to a student's t-test with a two-tailed distribution with heterodetic unequal variance for multiple comparisons.

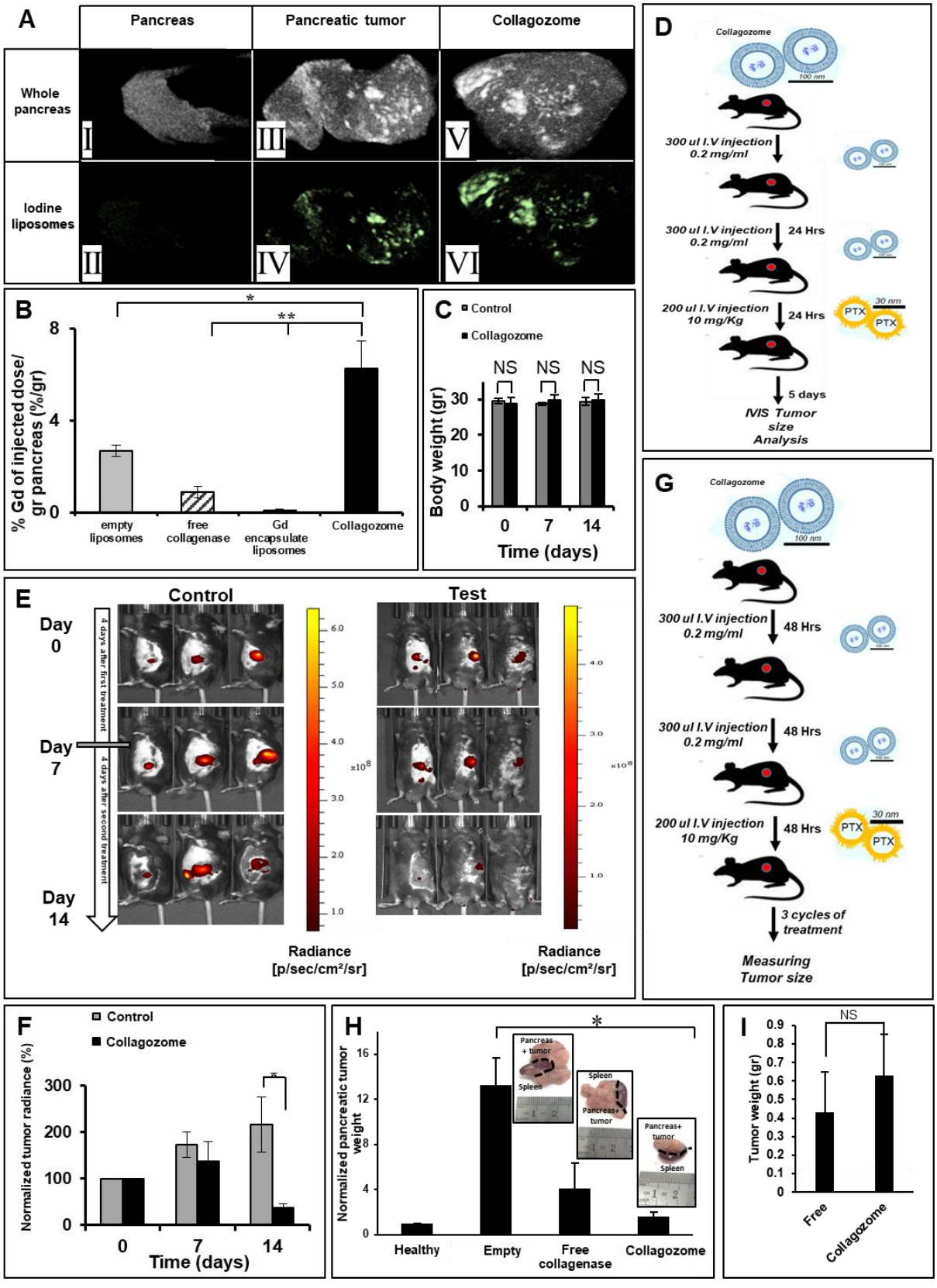
A
Pancreas
Pancreatic tumor
Collagozome
Whole pancreas
Iodine liposomes
I
II
III
IV
V
VI
B
% Gd of injected dose/ gr pancreas (%/gr)
empty liposomes
free collagenase
Gd encapsulate liposomes
Collagozome
C
Control
Collagozome
NS
Body weight (gr)
Time (days)
D
Collagozome
100 nm
300 ul I.V injection 0.2 mg/ml
300 ul I.V injection 0.2 mg/ml 24 Hrs
200 ul I.V injection 10 mg/Kg 24 Hrs
30 nm
PTX
5 days
IVIS Tumor size Analysis
E
Control
Test
Day 0
Day 7
Day 14
4 days after first treatment
4 days after second treatment
Radiance [p/sec/cm²/sr]
F
Control
Collagozome
Normalized tumor radiance (%)
Time (days)
G
Collagozome
100 nm
300 ul I.V injection 0.2 mg/ml 48 Hrs
200 ul I.V injection 10 mg/Kg 48 Hrs
30 nm
PTX
3 cycles of treatment
Measuring Tumor size
H
Normalized pancreatic tumor weight
Pancreas + tumor
Spleen
Pancreas+ tumor
Healthy
Empty
Free collagenase
Collagozome
I
NS
Tumor weight (gr)
Free
Collagozome

<u>Figure 3.</u> Enhanced pancreatic uptake after the collagozome pretreatment.

Collagozome pretreatment increased the pancreatic uptake of 100-nm liposomes. Iodine-loaded (A) or Gd-loaded (B) 100-nm liposomes were injected *intravenously* to mice bearing PDAC tumors, and the pancreases were imaged by CT; PDAC collagozome treatment group (A_{V-VI}) was compared to the non-treated PDAC group (A_{III-IV}) and to a control group (A_{I-II}). Similar quantitative results were recoded using Gd-liposomes and elemental analysis of the pancreas. (n=10 for the empty liposome group, n=5 of the free enzyme group, n=3 for the no pretreatment group and n=4 for the Collagozome treatment group).

Mice were administered 100-nm collagozome day after day, followed by a single dose of 30-nm paclitaxel-loaded micelles (10 mg/kg-body-weight) and the mCherry-expressing tumors were imaged. No major body-weight fluctuations were measured among the groups (C).

Therapeutic efficacy was recorded in mice pre-treated with collagozome followed by paclitaxel (D, E, F). Mice bearing PDAC tumors pretreated (right) or non-treated (left) with collagozome, 5 days after pretreatment were treated with paclitaxel micelles (D). Tumors were imaged over two weeks (E); tumor radiance decreased by 64% in the liposome (test) group and increased by 16% in the control (F). Results are representative of five biological replicates for both groups.

A schematic representation of the treatment protocol (G) Mice baring PDAC tumors were administered with 100-nm Collagozome, empty or free collagenase, in 48 hour gaps, followed by a single dose of 30-nm paclitaxel-loaded micelles (10 mg/kg-body-weight). This was repeated for 3 cycles with at least 3 mice in each experimental group.

Therapeutic efficacy was recorded in mice pre-treated with collagozome liposomes followed by paclitaxel (H). Mice bearing PDAC tumors were pretreated with either collagozome, empty liposomes or free liposomes followed by paclitaxel micelle treatment. Tumors were weighed at the end point. Values presented are relative to healthy pancreas size. (H). No change in tumor weight was observed between collagozome treated mice (without paclitaxel micelle treatment) compared to free collagozome (I).

*indicates *p*-value<0.05, **indicates *p*-value<0. All *P*-values presented were calculated between specified bars according to a student's t-test with a two-tailed distribution with heterodetic unequal variance for multiple comparisons.

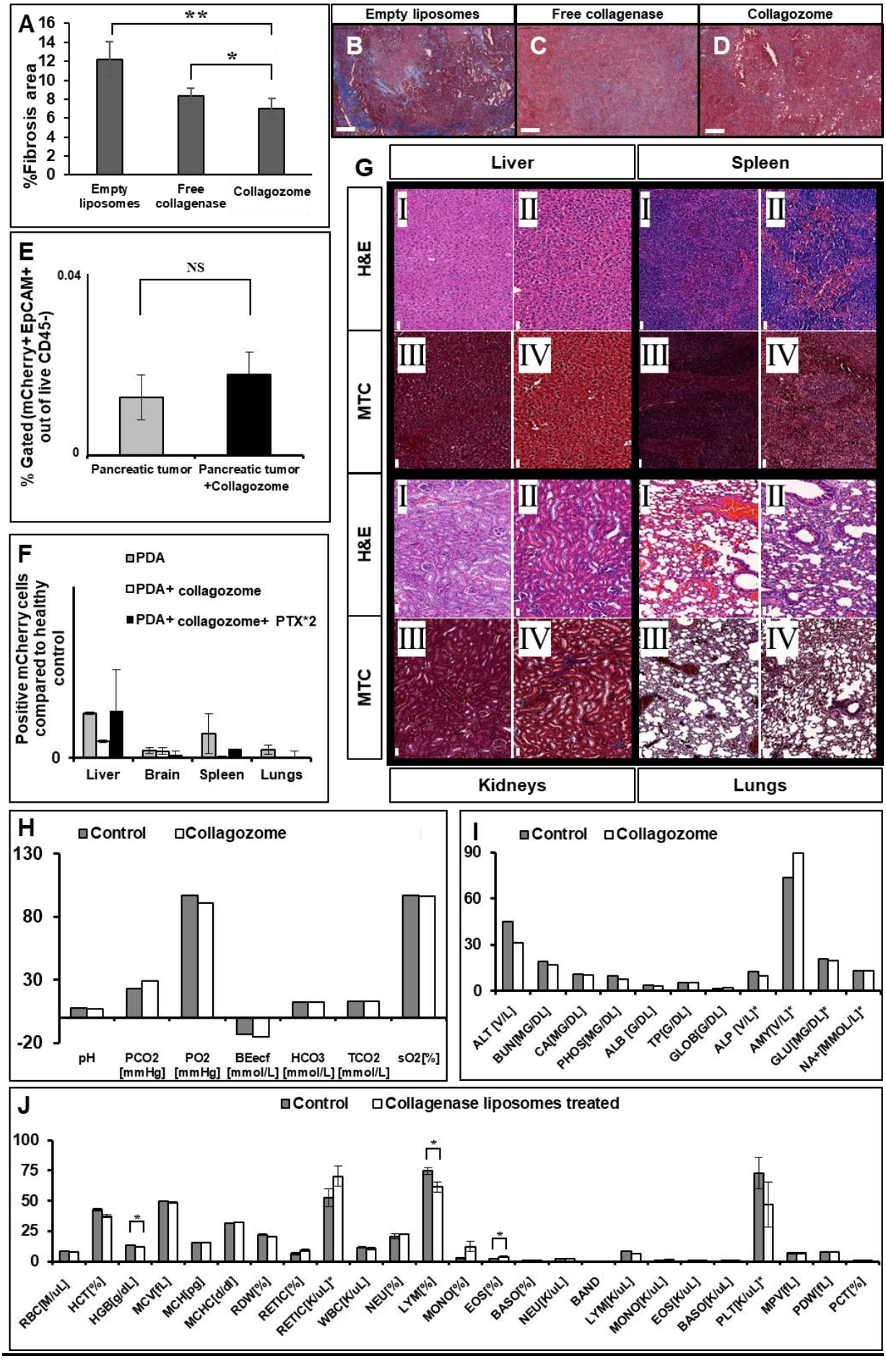
A
%Fibrosis area
16
14
12
10
8
6
4
2
0
**
*
Empty liposomes
Free collagenase
Collagozome
Empty liposomes
Free collagenase
Collagozome
B
C
D
E
% Gated (mCherry+EpCAM+ out of live CD45-)
0.04
0
NS
Pancreatic tumor
Pancreatic tumor +Collagozome
F
PDA
PDA+ collagozome
PDA+ collagozome+ PTX*2
Positive mCherry cells compared to healthy control
0
Liver
Brain
Spleen
Lungs
G
Liver
Spleen
H&E
MTC
H&E
MTC
I
II
III
IV
Kidneys
Lungs
H
Control
Collagozome
130
80
30
-20
pH
PCO2 [mmHg]
PO2 [mmHg]
BEecf [mmol/L]
HCO3 [mmol/L]
TCO2 [mmol/L]
sO2[%]
I
Control
Collagozome
90
60
30
0
ALT [V/L]
BUN[MG/DL]
CA[MG/DL]
PHOS[MG/DL]
ALB [G/DL]
TP[G/DL]
GLOB[G/DL]
ALP [V/L]*
AMY[V/L]*
GLU[MG/DL]*
NA+[MMOL/L]*
J
Control
Collagenase liposomes treated
100
75
50
25
0
*
*
*
RBC[M/uL]
HCT[%]
HGB[g/dL]
MCV[fL]
MCH[pg]
MCHC[d/dl]
RDW[%]
RETIC[%]
RETIC[K/uL]*
WBC[K/uL]
NEU[%]
LYM[%]
MONO[%]
EOS[%]
BASO[%]
NEU[K/uL]
BAND
LYM[K/uL]
MONO[K/uL]
EOS[K/uL]
BASO[K/uL]
PLT[K/uL]*
MPV[fL]
PDW[fL]
PCT[%]

<u>Figure 4</u>. Collagozome reduce collagen quantity in PDAC tumors (A-D)
Mice baring PDAC tumors were administered with either 100-nm empty liposomes (B), free collagenase (C), or collagozome (D), twice a week for three weeks. Pancreatic tumor sections were stained for collagen with Masson's Trichrome. Scale bar= 200μm. Quantification of Masson's Trichrome staining was done by Image J. Five sections were quantified for % collagen in tumor area in at least three mice of the same treatment (A).
Circulating tumor cells (CTCs) and tissue morphology after collagenase treatments histological evaluation of organs from *in-vivo* collagenase-treated and untreated mice (E).
H&E staining (I,II) Masson's Trichrome collagen staining (III,IV) of the liver, spleen, kidneys and lungs among the collagozome non-treated (odd numbers) and treated groups (even numbers). Results are representative of two biological replicates for both groups). Scale bar= 50μm.
Circulating tumor cells (CTCs) were measured in mice serum 24-hours after the collagenase treatment (F). No significant differences were observed between the PDAC-treated and the non-treated groups (n=4 for both groups).
NS indicates *p*-value>0.05 according to a Student's t-test with a two-tailed distribution with equal variance.
No evidence of metastatic disease was observed in the liver, brain, spleen and lungs 7 days after the collagenase treatment (G). Results are representative of 2 biological replicates for all groups. NS indicates *p*-value>0.05 according to a Student's t-test with a two-tailed distribution with unequal variance.
Comparing blood panels of collagozome treated and untreated mice: oxygen, chemistry and electrolyte analysis (H,I), red blood cell, reticulocyte, platelet count and white blood cell analysis (J) between the collagozome treated mice and non-treated mice 24 hours after the injection.
*indicates *p*-value<0.05 All *P*-values presented were calculated between specified bars according to a student's t-test with a two-tailed distribution with heterodetic unequal variance for multiple comparisons.

Materials and Methods

Collagenase liposomes, collagozomes

Collagenase type-I (Sigma-Aldrich, St. Louis, MO, USA) was encapsulated in 100-nm liposomes. A lipid mixture of 1,2-dimyristoyl-sn-glycero-3-phosphocholine (DMPC; Avanti Polar Lipids, Alabaster, AL, USA), cholesterol (Sigma-Aldrich) and 1,2-distearoyl-sn-glycero-3-phosphoethanolamine-N-methoxy-polyethylene glycol 2000 (PEG-DSPE; Avanti), at three different molar ratios of: 95:0:5, 80:15:0 and 56:39:5, respectively, were dissolved in absolute ethanol. The lipid solution was added to calcium free Dulbecco's Phosphate Buffer Saline (PBS; Sigma-Aldrich) solution containing 2mg/ml collagenase to reach a lipid concentration of 50mM, at 50°C. The liposomes were downsized using a Lipex extruder (Northern Lipids, Vancouver, Canada) five times through each 400, 200 and 100-nm polycarbonate etched membrane (Whatman, Newton, MA, USA) at 40°C with a maximal working pressure of 10bar. The non-encapsulated protein was removed by dialysis using a 1000kDa cutoff membrane (Spectrum Labs, CA, USA) against PBS solution (1:1000 vol ratio); the external PBS was replaced after 1, 3 and 24 hours, at 4°C. Liposomes were sized using a Zetasizer NanoZSP (Malvern Instruments, Worcestershire, UK) using disposable polystyrene cuvettes after diluting the samples 1:100 in PBS.

Collagenase encapsulation measurement. Collagozome was dissociated using 1% triton-x100 in PBS. The mixture was placed in an Eppendorf shaker at 55°C at 300rpm for 15 minutes to dissociate the liposomes. The mixture was centrifuged for 10 minutes at 12,000rpm at 4°C. The liposome-free supernatant was collected and centrifuged again for 10 minutes at 12,000rpm at 4°C. The protein concentration was determined using a **MicroBCA Protein Assay**

Kit (ThermoFisher Scientific, MA, USA). Protein concentration was measured by absorbance at 562nm using the Infinite 200PRO multimode reader (TECAN, Mannedorf, Switzerland). Encapsulation efficiency reached 10% which is equivalent to collagenase concentration of 0.2 mg/ml inside the liposomes.

A second determination method was done by **Fluorescamine**. Collagozomes were dissociated with the same method as done for BCA. Fluorescamine was diluted to 0.75mg/ml final concentration when added to liposomal sample. The fluorescence was then determined using Infinite 200PRO multimode reader (TECAN, Mannedorf, Switzerland) with a 400 nm, 30 nm bandwidth, excitation filter and a 460 nm, 40 nm bandwidth emission filter. Protein concentration was calculated based on BSA (bovine serum albumin) calibration curve.

Collagenase activity assay. Collagenase type-I activity was determined using gelatin with fluorescein conjugate as a substrate (ThermoFisher). Collagenase (100μl) was mixed with 80μl of reaction buffer (0.05M Tris-HCl, 0.15M NaCl, 5mM CaCl2, and 0.2mM sodium azide at pH 7.6) and 20μl of 0.125mg/ml gelatin diluted in PBS. Following 1 hour incubation of liposomes at 37°C The fluorescent intensity was measured every 15 seconds over a period of 3 minutes at 485nm and 530nm (excitation/emission) using an Infinite 200PRO. Collagenase activity was measured at 37°C, where plasma or PBS served as control.

Collagenase release profile. Collagenase release from the liposomes was measured using dialysis tubes 1000kDa molecular cutoff (SpectraPor) against PBS (1:15 vol ratio) at 37°C with 100rpm shaking. Triplicates vials were used for each liposome formulation. The released protein concentration was determined using MicroBCA Protein Assay Kit (ThermoFisher).

Gd-rhodamine liposomes Gadolinium diethylenetriaminepentaacetate (Gd; Sigma-Aldrich) was incorporated into 100-nm liposomes. A lipid mixture of hydrogenated soybean phosphatidylcholine (HSPC; Avanti) cholesterol (Sigma-Aldrich), 1,2-dipalmitoyl-sn-glycero-3-phosphoethanolamine-N-(lissamine rhodamine B sulfonyl (Rhod-DSPE; Avanti) and PEG-DSPE (Avanti) at a molar ratio of 55.94:39:0.06:5 respectively were dissolved in absolute ethanol at 70°C. The dissolved lipids were quickly injected into a PBS solution containing 270 mg/ml of Gd, at 70°C, to reach a lipid concentration of 50mM. The liposomes were extruded five times through 100-nm polycarbonate membranes (Whatman) at 70°C. The free Gd was removed by dialysis in a 12-14kDa membrane (Spectrum Laboratories) against PBS solution at 4°C for 24 hours. Liposomes were sized using a Zetasizer NanoZSP (Malvern).

Gd release profile. Gd release profile from the liposomes was measured by dialysis using 14kDa cutoff membrane (SpectraPor) loaded with the Gd-liposomes against PBS at a 1:15 vol ratio at 37°C and 100rpm shaking. Released Gd was measured using the elemental analysis 5110 ICP-OES (Agilent, CA, USA) at wavelengths of 335.048 and 342.246nm.

Gd Liposome concertation measurements. Gd-liposome' concentration (liposomes/ml) was measured using a NanoSight NS300 (Malvern, Worcestershire, UK) equipped with a sCMOS camera. Slider shutter and gain were set to 1206 units and 366 respectively, total number of 749 frames were captured with 25 frames per second rate. The temperature was set to 24.4°C.

Gd-rhodamine liposome biodistribution. Mice bearing PDAC, 6 weeks after the initiation of the tumor model were administered, *via* tail vein injection, 400µl of 1.2 mg/ml Gd-liposomes. Mice were sacrificed at different time intervals: 1, 8, 14- and 24-hours post

administration and their organs were collected. Tissues were combusted for 5 hours at 550°C and then dissolved in 1%vol nitric acid. Gadolinium in each organ was quantified using ICP-EOS (Agilent) at wavelengths of 335.048 and 342.246nm.

Differential Scanning Calorimetry. DSC measurements were performed using a NanoDSC (TA Instruments, New Castle, DE, USA). Liposome suspensions were measured at temperatures ranging from 10 to 65°C with intervals of 0.5 °C/min. PBS was used as a reference buffer.

Tissue culture

KPC cells were established in the laboratory of Surinder K. Batra. KPC cells were LSL-KrasG12D/+;LSL-Trp53R172H/+ of pancreatic carcinomas, along with inactivation of the ;Pdx-1-Cre mice [60] (KPC) transgenic mice.[61] Cells were cultured in Dubalco Modified Eagle's medium (DMEM; SigmQa-Aldrich) supplemented with 10% fetal bovine serum (FBS, Biological Industries, CT, USA), 100 IU ml-1 Penicillin, 100 µg ml-1 Streptomycin and 2 mM L-glutamine (Biological Industries) and grown at 37°C; 5% CO_2. KPC cells expressing the fluorescent protein mCherry were developed by the Satchi-Fainaro Laboratory at the Tel Aviv University, and cultured in DMEM medium, supplemented with 10% fetal bovine serum1% 2mML-glutamine and 1% 100U penicillin with 0.1 mg/ml streptomycin or 10 µg/ml of puromycin at 37°C and 5% CO2. All cells tested negative for mycoplasma (EZ-PCR, Mycoplasma test kit, Biological industries).

PDAC model

All the animal studies were approved by, and complied with, the institutional and ethical committee at the Technion. Animals' well-being was monitored daily by certified veterinarians at the Technion facility.

Several mouse models have been developed to study pancreatic cancer,[62] each with its similarities and differences to the disease manifestations in humans. Here, we chose to test our approach on C57BL/6 mice bearing KPC (LSL-KrasG12D/+;LSL-Trp53R172H/+ of pancreatic carcinomas) tumors[60, 61] implanted orthotopically in the pancreas. Specifically, these tumors resemble human pancreatic adenocarcinoma in their excess expression of extracellular collagen.

Ten-week-old C57BL/6 mice (Harlan Laboratories, Jerusalem, Israel) were anesthetized using Ketamine/Xylazine (100mg/kg and 10mg/kg-bodyweight, respectively) injected *intraperitoneally*. A subcutaneous injection of 0.05 mg/kg buprenorphine was performed before the surgery. The mice were placed on 37°C warmed pads. The lateral, abdominal left side of the mice was shaved, and a 1-cm longitudinal cut was performed above the pancreas in the skin. While observing the spleen and the pancreas 1-cm cut was done in the *peritoneum.* The pancreas was then secured using forceps. 250,000 KPC-mCherry cells were suspended in 0.01ml at 4°C PBS and were injected using 5µl Hamilton syringe with 30G at 30 degrees using a point style 4 needle (Hamilton, NV, USA) to the pancreas.[63] Cuts were sutured using 5-0 degradable sutures (Vicryl, AR, USA).

Liver fibrosis model

Six weeks old Balb/c mice (Harlan Laboratories, Jerusalem, Israel) were anesthetized with isoflurane (4% induction, 2% maintenance inhaled) and injected *intraperitoneally* in chemical hood tri-weekly with 2ml/Kg Carbon tetrachloride (Sigma- Aldrich) diluted in olive oil for 2 weeks (6 injections) [41-44].

Collagen analysis after the collagenase treatment.

Pancreatic tumors and were harvested from tumor bearing mice, six weeks after the initiation of the tumor model. Each tumor was sliced horizontally to 1cm thick slices. All the extracted slices were mixed and randomly chosen for different treatments groups. Treatments included incubation in DMEM medium (Sigma-Aldrich) with collagenase type-I (Sigma-Aldrich) at increasing concentrations: 0.05, 0.1 or 0.2 mg/ml for either 8 or 24 hours. Following the enzymatic treatment, the tumor slices were sectioned, fixated in 10% formalin (Sigma-Aldrich) and stained with Masson's Trichrome. Computerized morphometry (by Image J) was utilized to quantitate the fraction of the fibrotic area out of the total area of the tumor in each sample. Computerized morphometry of the collagen was used to determine fibrosis fraction within each tumor sample. Masson's Trichrome staining was performed to identify the pancreatic fibrosis. Then, stained slides were entirely scanned at magnification of X20 using the Panoramic MIDI automatic digital slide scanner (3DHistech, Budapest, Hungary). The whole slide was analyzed in Image Pro Premier 9.2 software (Media Cybernetics, MD, USA). Tumor fibrosis area was calculated according to the blue staining within the tumor tissue, and the tissue area was calculated by choosing the whole tissue with the machine 'color picker tool' (Image J). The same procedure was done to mice's livers following liver fibrosis induction.

The effect of the collagenase treatment on pancreatic uptake of Gd-liposomes. Mice were treated with two injections of collagozome 24 hours apart (n=4 mice). Control groups included injections of empty liposomes (n=10 mice), free collagenase (n=5 mice) or no injection at all (n=3 mice) instead of collagozomes. Twenty-four hours after the second treatment, 400µl of Gd-liposomes were injected *intravenously* to the tail vein. 24 hours later, the animals were euthanized, and their organs were harvested. The amount of Gadolinium in each

organ was analyzed using elemental analysis (ICP-EOS, Agilent) at wavelengths of 335.048 and 342.246nm. The organs were harvested, weighed and then burnt at 550°C overnight. The burnt organs were dissolved in 5 ml of 1% nitric-acid and filtered using 22µm filters (Millipore Millex-GV, Merck, Darmstadt, Germany). The Gd concentration in the organs was measured using an ICP-EOS elemental analysis.

In-vivo imaging

***Intra-vital* microscopy.** Mice were anesthetized using ketamine/xylazine. 300µl of Gd-rhodamine liposomes were injected *intravenously* to the tail vein. One-hour after the injection, a 1-cm incision was performed above the pancreas. An SZX16 microscope equipped with a CY3 filter and SDF PLAPO 0.5X PF lens (Olympus, PA, USA) was used at an exposure time of 365ms; the threshold was determined by the auto-fluorescence of the healthy pancreas. Image editing of +20% brightness and contrast was performed.

MRI hardware and animal monitoring. Magnetic resonance imaging (MRI) was performed using a 9.4T bore scanner (Bruker Biospec, Ettlingen, Germany), equipped with a Transmit/Receive cylindrical volume coil (72 mm inner diameter). Animals were anesthetized using 0.5-1.5% isoflurane, supplemented with oxygen (0.7 l/min). Respiration was monitored during imaging (Small Animal Instruments, Stony Brook, NY, USA) and body temperature was maintained using thermostat-regulated circulating hot water. T2-weighted images were first obtained to identify the pancreas location using a RARE sequence with respiratory gating (0.6mm thickness, 25 slices, FOV=6x3cm, matrix dimension=256x128, TR/TE=600/16.2ms, 3 averages). Gd-liposomes were imaged using T1-weighted RARE sequence with respiratory

gating (0.6mm thickness, 13 slices, FOV=6x3cm, matrix dimension=256x128, TR/TE=1200/16.2ms, 3 averages), sequences were acquired every 2 min over 25 min.

Micro-CT scan. Mice were imaged using an IVIS Spectrum CT Pre-clinical *in-vivo* imaging system (PerkinElmer, MA, USA) with the following parameters: CT was set to 50ms, total projections were 720, voltage was set to 50kV while the current to 1mA the binning was determined to 2 and the X-ray filter was set to 440 A1. Hounsfield calibration was performed in air-0.004168 and water-0.5513. Two groups of tumors bearing mice (n=5 each) were divided to control and test group. The mice were weighed weekly and tumor progression was monitored by weekly IVIS scans (PerkinElmer). Epi-fluoresce scans were acquired under the following parameters: excitation 570nm, emission 620nm, at 3 seconds exposure. Therapeutic treatment began four weeks after the initial tumor cells injection. The test group received 300µl dose of collagozomes for two consecutive days, while the control group remained untreated. On the third day, both groups received a single dose of 10 mg/kg micellar paclitaxel.[19] Tumor dimensions were assessed using the ROI tool in the IVIS imaging software (Living Image, PerkinElmer).

Micro-ultrasound tumor imaging Mice were anesthetized with 2% isoflurane and kept at 37^{o}C. The tumor imaging was performed using a Vevo2100 Micro-ultrasound imaging system (Visualsonics) equipped with13-38MHz (MS 400) and 22-55MHz (MS550D) array transducers. Conventional two-dimensional imaging recordings were performed to determine tumor size.

PDACs' ECM SEM scanning. For SEM images, the pancreas samples were divided into three groups: treated, cancerous and non-cancerous. Then, each pancreas was cut into small pieces and decellularized by 2-24 hours rounds agitation in a 1% sodium dodecyl sulfate (Sigma-Aldrich) and 0.1% Penicillin/Streptomycin (Biological Industries) in PBS.[64] Subsequently, the

samples were washed in distilled water, lyophilized and sputter-coated with gold in a Polaron E5100 coating apparatus (Quorum technologies, Lewis, UK) and observed under JSM-840A SEM (JEOL, Tokyo, Japan).

Paclitaxel micelles. All substances used for polymerization, specifically methyl trifluoromethylsulfonate (MeOTf) was refluxed over CaH_2 2-n-buty-2-oxazoline (BuOx) and benzonitrile (PhCN) were refluxed over P_2O_5 and distilled and stored under argon. The polymerization and work-up procedures were carried out as described previously.[65] Briefly, 1.91 g (11.6 mmol; 1 eq) MeOTf was added to a dried and nitrogen flushed flask and dissolved in 250 mL PhCN. 34.6 g (407 mole; 35 eq) of 2-methyl-2-oxazoline (MeOx) was added and the reaction mixture was heated to 100°C for 4 hours. Reaction progress was controlled by FTIR- and 1H-NMR-spectroscopy. After complete consumption of MeOx, the mixture was cooled to RT and 29.4 g (232 mole; 20 eq) 2-n-butyl-2-oxazoline (BuOx) was added. The reaction mixture was heated to 100°C overnight. The procedure was repeated with 34.6 g (407 mole; 35 eq) MeOx and termination was carried out with 3.0 g (35.2 mmol; 3 eq) piperidine (Pip) at 50°C for 4 hours. Subsequently, 1.92 g (13.9 mmole; 1 eq) of K_2CO_3 was added and the mixture was stirred at 50°C for 4 hours. Precipitates were removed by centrifugation and the solvent removed under reduced pressure. The supernatant was transferred into a dialysis bag (MWCO 1 kDa, cellulose acetate) and dialyzed against Millipore water overnight. The solution was recovered from the bag and lyophilized. Drug loaded polymer micelles were prepared using the thin film method (Figure S5).[24] Ethanolic polymer (50 g/L) and paclitaxel (20 g/L) stock solutions were mixed in desired ratio. After complete removal of the solvent at 55°C, the films were dried further *in vacuo* (≤ 0.2 mbar) overnight. Subsequently, preheated (37°C) H_2O (Millipore) was added to obtain final polymer and drug concentrations of P2/PTX = 50/40 g/L. Complete solubilization was

facilitated by shaking the solutions at 55 °C for 30 min. Non-solubilized drug (if any) was removed by centrifugation for 5 min at 10.000 rpm with a Universal 320 R centrifuge, *Hettich* (Tuttlingen, Germany).

Detection of circulating tumor cells (CTCs) from mouse blood by Flow Cytometry. Blood was sampled from the facial vein of mice from 3 different groups: (i) normal, (ii) mCherry-labeled tumor-bearing mice and (iii) mCherry-labeled tumor-bearing mice treated with liposomes (n = 4 mice per group). Blood (20 µl) was collected into an anticoagulant (EDTA)-containing tube, diluted 1:5 with PBS (Sigma-Aldrich) and incubated with anti-mouse CD326 (EpCAM) APC eFlour 780 (cat#47-5791-80, eBioscinces, 0.125µg per sample) and anti-mouse CD45 FITC (cat#11-0451-82, eBioscinces, 0.5µg per sample) for 1 hour at room temperature protected from light. Blood samples were diluted with PBS 1:10 (vol ratio) and DAPI 5 µg/ml was added. CTCs in diluted blood samples were detected using flow cytometry (Attune NxT, Life Technologies, ThermoFisher) and analyzed with Kaluza (Beckman Coulter, IN, USA) software. Briefly, mCherry signal and monoclonal antibodies were used to detect mCherry-labeled CTCs population with the following phenotype: mCherry+/EpCAM+/CD45-. DAPI was used to distinguish apoptotic and dead cells from viable cells. After acquisition of at least 300,000 cells per sample (whole sample was run) analyses were done on singlet cells. Percentages of live cells with the phenotype mCherry+/EpCAM+/CD45-is shown. Positive staining was defined as being greater than non-specific background staining and was verified on blood sample that was spiked-in with mCherry-labeled cells.

Metastasis detection. Mice were sacrificed, and the brain, lungs, liver and spleen were extracted and held in culture media (Roswell Park Memorial Institute medium; Sigma-Aldrich) at

4°C until initiating the organ's dissociation. Subsequently, the organs were enzymatically and physically dissociated using a GentleMacs machine (Miltenyi Biotec, Bergisch Gladbach, Germany) and tumor mouse dissociation kit (Miltenyi Biotec) following the machine dissociation protocols. Single cell suspension was obtained by passing the suspension in 70µm cell strainer (BD Biosciences, CA, USA). After dissociating the organs into a single-cell suspension, the mCherry KPC cells were detected in the mCherry channel, after acquisition of at least 100,000 cells per sample using a flow activated cell sorter (FACS; FACSARIA III, BD Biosciences) and analyzed with Diva (BD Biosciences) software. Proper gates of single cells and positive populations were obtained prior to the analysis.

Blood panels

Tumor-bearing mice (n=4 mice per group) were divided to control not treated and test groups. The test group treated by two consecutive, day after day, collagozomes 300µl *intravenous* injections. 24 hours after the second collagozomes injection blood was collected from the groups, 65µl from each mouse, and the samples were kept in 1ml lithium heparin and 0.5ml k3EDTA tubes. Analysis was performed using: VetscanVs2 (Abaxis, CA, USA), i-STAT portable clinical analyzer (Abaxis) and ProCyte Dx* Hematology Analyzer (IDEXX, Maine, USA).

Histology

Mice were euthanized at the sampling day. Tumors were extracted and kept in 10% natural buffer formalin (Sigma-Aldrich) at 4°C for 24 hours before they were paraffin embedded. The slides were deparaffinized and soaked in xylene for 3 minutes, xylene:ethanol 1:1 (vol ratio) for 3 minutes, absolute ethanol for 3 minutes, 95% ethanol for 3 minutes, 70% ethanol for 3 minutes, 50% ethanol for 3 minutes and then rinsed with tap water. Nuclei blue fluorescent staining was performed using NucBlue Fixed Cell ready probes (ThermoFisher) that was added for 10

minutes followed by rinsing with tap water. Hematoxylin and eosin (H&E) and Masson's Trichrome (MTC) staining for collagen evaluation was performed.

Fluorescent histology. The stained slides were scanned and analyzed using a 3D Histech Panoramic MIDI scanner (3D Histech, Budapest, Hungary) using an X20 objective magnification, exposure times of 100 msec for the DAPI channel, and 350 msec for the CY3 channel. Images were analyzed using an Image J Analysis software program to evaluate the levels of rhodamine in the tissue. Image editing of +40% brightness and contrast was done.

mRNA Extraction mRNA was purified using an Aurum total RNA fatty and fibrous tissue kit (#732-6830, Bio-Rad) according to the manufacturer's protocol. mRNA was quantified by measuring Ab260 nm with a NanoQuant plate in Infinite 200PRO multimode reader (TECAN, Mannedorf, Switzerland).

Quantitative Real Time PCR (RT-qPCR) cDNA was synthesized from mRNA samples using 400 ng of RNA in a 20µl total reaction mix of High-quality cDNA synthesis Kit (qPCRBIO) Biosystems). Real-time PCR was performed qRTPCR CFX Bio-Rad equipment with qPCRBIO Fast qPCR SyGreen Blue Mix, Hi-ROX, (qPCRBIO). Values were normalized with GAPDH expression levels. The primer sequences are:

GAPDH	F- TTGCCATCAACGACCCCTTCAT
	R- AGACTCCACGACATACTCAGCA
Collagen type 3α (col3α)	F- CTGTAACATGGAAACTGGGGAAA
	R-CCATAGCTGAACTGAAAACCACC

Smooth muscle actin (SMA) F- GTCCCAGACATCAGGGAGTAA

R- TCGGATACTTCAGCGTCAGGA

Supporting Information

Supporting information is available online. NanoSight 100-nm PEGylated nanoparticle measurements of the particle concentration and characterization of particles for zeta and drug to lipid ratio (Supplementary Figure S1) with calculation of nanoparticle biodistribution explained in Table S1. Detailed measurements of the three different collagenase concentrations (0.05, 0.1 and 0.2 mg/ml) that were tested *ex-vivo* over two times intervals (8 and 24 hours) (Supplementary Figure S2). Elemental ICP-OES analysis of organs of mice that were pretreated with collagozome, free collagenase or empty liposomes and then injected intravenously with gold nanoparticles at various sizes (5,20,100nm) to asses biodistribution following pretreatment in healthy (Supplementary Figure S3) and PDAC (mice Supplementary Figure S4) .Micro-ultrasound image to describe how tumor measurement were performed *in vivo* (Supplementary Figure S5).DLS 30-nm measurement for paclitaxel micelles.

Acknowledgments

This work was supported by ERC-STG-2015-680242.

The authors also acknowledge the support of the Technion Integrated Cancer Center (TICC), the Russell Berrie Nanotechnology Institute, the Lorry I. Lokey Interdisciplinary Center for Life Sciences & Engineering, the Pre-Clinical Research Authority staff and the Biomedical Core Facility at the Rappaport Faculty of Medicine, as well as the Israel Ministry of Economy for a Kamin Grant (52752); the Israel Ministry of Science Technology and Space – Office of the Chief Scientist (3-11878); the Israel Science Foundation (1778/13, 1421/17); the Israel Cancer

Association (2015-0116); the German-Israeli Foundation for Scientific Research and Development for a GIF Young grant (I-2328-1139.10/2012); the European Union FP-7 IRG Program for a Career Integration Grant (908049); the Phospholipid Research Center Grant; a Mallat Family Foundation Grant; A. Schroeder acknowledges Alon and Taub Fellowships. A. Zinger acknowledges a generous fellowship form the Technion Russell Berrie Nanotechnology Institute (RBNI). N. Krinsky wishes to thank the Baroness Ariane de Rothschild Women Doctoral Program for its generous support. O. Adir wishes to thank the Sherman and Gutwirth Interdisciplinary Graduate School Fellowships. M. Poley wishs to thank the Ministry of Science and Technology for the Shulamit Aloni Doctoral Fellowship. R. Luxenhofer acknowledges support by the Deutsche Forschungsgemeinschaft (Project number 398461692) and M.M. Lübtow would like to thank the Evonik Foundation for providing a doctoral fellowship. The authors also acknowledge Dr. R. Shofty, Dr. D. Levin-Ashkenazi, Ms. V. Zlobin, Mr. N. Amit from the Technion Pre-Clinical Research Authority for their help with the *in-vivo* animal tests. Mr. Dima Zagorski and Mrs. Keren Filhart for the graphical aid and Dr. E. Suss Toby, Dr. E. Messer, Mrs. M. Holdengreber and Ms. O. Schwartz from the Bioimaging Center at the Technion Faculty of Medicine, for their assistance with imaging and image analysis.

The help of Mrs Julie Bloch Mendelsohn JD, MPH in editing this manuscript is greatly appreciated.

References

1. Olive, K. P.; Jacobetz, M. A.; Davidson, C. J.; Gopinathan, A.; McIntyre, D.; Honess, D.; Madhu, B.; Goldgraben, M. A.; Caldwell, M. E.; Allard, D.; Frese, K. K.; Denicola, G.; Feig, C.; Combs, C.; Winter, S. P.; Ireland-Zecchini, H.; Reichelt, S.; Howat, W. J.; Chang, A.; Dhara, M. *et al.*, Inhibition of Hedgehog Signaling Enhances Delivery of Chemotherapy in a Mouse Model of Pancreatic Cancer. *Science* **2009,** *324* ,1457-1461.

2. Schuerle, S.; Soleimany, A. P.; Yeh, T.; Anand, G. M.; Haberli, M.; Fleming, H. E.; Mirkhani, N.; Qiu, F.; Hauert, S.; Wang, X.; Nelson, B. J.; Bhatia, S. N., Synthetic and Living Micropropellers for Convection-Enhanced Nanoparticle Transport. *Sci. Adv.* **2019,** *5*, eaav4803.

3. Neesse, A.; Algul, H.; Tuveson, D. A.; Gress, T. M., Stromal Biology and Therapy in Pancreatic Cancer: A Changing Paradigm. *Gut* **2015,** *64*, 1476-1484.

4. Molinaro, R.; Corbo, C.; Livingston, M.; Evangelopoulos, M.; Parodi, A.; Boada, C.; Agostini, M.; Tasciotti, E., Inflammation and Cancer: In Medio Stat Nano. *Curr. Med. Chem.* **2018** ;25:4208-4422.

5. Provenzano, P. P.; Cuevas, C.; Chang, A. E.; Goel, V. K.; Von Hoff, D. D.; Hingorani, S. R., Enzymatic Targeting of the Stroma Ablates Physical Barriers to Treatment of Pancreatic Ductal Adenocarcinoma. *Cancer Cell* **2012,** *21*, 418-429.

6. Friedman, S. L., Liver Fibrosis–from Bench to Bedside. *J. Hepatol.* **2003,***38*, 38-53.

7. Venditto, V. J.; Szoka, F. C., Cancer Nanomedicines: So Many Papers and So Few Drugs! *Adv. Drug. Delivery Rev.* **2013,** *65*, 80-88.

8. Kohli, A. G.; Kivimäe, S.; Tiffany, M. R.; Szoka, F. C., Improving the Distribution of Doxil® in the Tumor Matrix by Depletion of Tumor Hyaluronan. *J. Controlled Release* **2014,** *191*, 105-114.

9. Mahadevan, D.; Von Hoff, D. D., Tumor-Stroma Interactions in Pancreatic Ductal Adenocarcinoma. *Mol. Cancer Ther.* **2007,** *6*, 1186-1197.

10. Kozono, S.; Ohuchida, K.; Eguchi, D.; Ikenaga, N.; Fujiwara, K.; Cui, L.; Mizumoto, K.; Tanaka, M., Pirfenidone Inhibits Pancreatic Cancer Desmoplasia by Regulating Stellate Cells. *Cancer Res.* **2013**, 73, 2345-2356.

11. Wang-Gillam, A., Targeting Stroma: A Tale of Caution. *J. Clin. Oncol.* **2019**, 37, 1041-1043.

12. Gilpin, D.; Coleman, S.; Hall, S.; Houston, A.; Karrasch, J.; Jones, N., Injectable Collagenase Clostridium Histolyticum: A New Nonsurgical Treatment for Dupuytren's Disease. *J .Hand. Surg. Am.* **2010,** *35*, 2027-2038.

13. Li, X.; Ma, Q.; Xu, Q.; Duan, W.; Lei, J.; Wu, E., Targeting the Cancer-Stroma Interaction: A Potential Approach for Pancreatic Cancer Treatment. *Curr. Pharm. Des.* **2012,** *18*, 2404-2415.

14. Bond, M. D.; Van Wart, H. E., Characterization of the Individual Collagenases from Clostridium Histolyticum. *Biochemistry* **1984,** *23*, 3085-3091.

15. Mandl, I.; Zipper, H.; Ferguson, L., Clostridium Histolyticum Collagenase: Its Purification and Properties. *Arch. Biochem. Biophys.* **1958,** *74*, 465-475.

16. Nagase, H.; Visse, R.; Murphy, G., Structure and Function of Matrix Metalloproteinases and Timps. *Cardiovasc. Res.* **2006,** *69*, 562-573.

17. Zhang, X.; Zhang, K.; Haag, R., Multi-Stage, Charge Conversional, Stimuli-Responsive Nanogels for Therapeutic Protein Delivery. *Biomater. Sci.* **2015,** *3*, 1487-1496.

18. Evangelopoulos, M.; Tasciotti, E., Bioinspired Approaches for Cancer Nanotheranostics. *Nanomedicine* **2017**, 12, 5-7.

19. Luxenhofer, R.; Schulz, A.; Roques, C.; Li, S.; Bronich, T. K.; Batrakova, E. V.; Jordan, R.; Kabanov, A. V., Doubly Amphiphilic Poly (2-Oxazoline) S as High-Capacity Delivery Systems for Hydrophobic Drugs. *Biomaterials* **2010,** *31*, 4972-4979.

20. Von Hoff, D. D.; Ervin, T.; Arena, F. P.; Chiorean, E. G.; Infante, J.; Moore, M.; Seay, T.; Tjulandin, S. A.; Ma, W. W.; Saleh, M. N., Increased Survival in Pancreatic Cancer with Nab-Paclitaxel Plus Gemcitabine. *N. Engl. J. Med.* **2013,** *369*, 1691-1703.

21. Patra, C. R.; Bhattacharya, R.; Mukhopadhyay, D.; Mukherjee, P., Fabrication of Gold Nanoparticles for Targeted Therapy in Pancreatic Cancer. *Adv. Drug Delievery Rev.* **2010,** *62*, 346-361.

22. Cabral, H.; Matsumoto, Y.; Mizuno, K.; Chen, Q.; Murakami, M.; Kimura, M.; Terada, Y.; Kano, M.; Miyazono, K.; Uesaka, M., Accumulation of Sub-100 Nm Polymeric Micelles in Poorly Permeable Tumours Depends on Size. *Nat. Nanotechnol.* **2011,** *6*, 815-823.

23. Pittella, F.; Miyata, K.; Maeda, Y.; Suma, T.; Watanabe, S.; Chen, Q.; Christie, R. J.; Osada, K.; Nishiyama, N.; Kataoka, K., Pancreatic Cancer Therapy by Systemic Administration of Vegf Sirna Contained in Calcium Phosphate/Charge-Conversional Polymer Hybrid Nanoparticles. *J. Controlled Release* **2012,** *161*, 868-874.

24. Nishiyama, N.; Matsumura, Y.; Kataoka, K., Development of Polymeric Micelles for Targeting Intractable Cancers. *Cancer Sci.* **2016,** *107*, 867-874.

25. Min, H. S.; Kim, H. J.; Ahn, J.; Naito, M.; Hayashi, K.; Toh, K.; Kim, B. S.; Matsumura, Y.; Kwon, I. C.; Miyata, K.; Kataoka, K., Tuned Density of Anti-Tissue Factor Antibody Fragment onto Sirna-Loaded Polyion Complex Micelles for Optimizing Targetability into Pancreatic Cancer Cells. *Biomacromolecules* **2018,** *19*, 2320-2329.

26. Yang, F.; Jin, C.; Jiang, Y.; Li, J.; Di, Y.; Ni, Q.; Fu, D., Liposome Based Delivery Systems in Pancreatic Cancer Treatment: From Bench to Bedside. *Cancer Treat. Rev.* **2011,** *37*, 633-642.

27. Yu, M. K.; Jeong, Y. Y.; Park, J.; Park, S.; Kim, J. W.; Min, J. J.; Kim, K.; Jon, S., Drug-Loaded Superparamagnetic Iron Oxide Nanoparticles for Combined Cancer Imaging and Therapy *In Vivo*. *Angew. Chem.* **2008,** *120*, 5442-5445.

28. Schroeder, A.; Heller, D. A.; Winslow, M. W.; Dahlman, J. E.; Pratt, G. W.; Langer, R.; Jacks, T.; Anderson, D. G., Treating Metastatic Cancer with Nanotechnology. *Nat. Rev. Cancer* **2011,** *12*, 39-50.

29. Israelachvili, J. N., *Intermolecular and Surface Forces*. 2 ed.; Academic Press: London, 1992.

30. Pandol, S.; Edderkaoui, M.; Gukovsky, I.; Lugea, A.; Gukovskaya, A., Desmoplasia of Pancreatic Ductal Adenocarcinoma. *Clin. Gastroenterol. Hepatol.* **2009,** *7*, S44-S47.

31. Mollenhauer, J.; Roether, I.; Kern, H., Distribution of Extracellular Matrix Proteins in Pancreatic Ductal Adenocarcinoma and Its Influence on Tumor Cell Proliferation *In Vitro*. *Pancreas* **1987,** *2*, 14-24.

32. Talmi-Frank, D.; Altboum, Z.; Solomonov, I.; Udi, Y.; Jaitin, D. A.; Klepfish, M.; David, E.; Zhuravlev, A.; Keren-Shaul, H.; Winter, D. R., Extracellular Matrix Proteolysis by Mt1-Mmp Contributes to Influenza-Related Tissue Damage and Mortality. *Cell Host Microbe* **2016,** *20*, 458-470.

33. Koynova, R.; Caffrey, M., Phases and Phase Transitions of the Phosphatidylcholines. *Biochim. Biophys. Acta, Biomembr.* **1998,** *1376*, 91-145.

34. Zinger, A.; Adir, O.; Alper, M.; Simon, A.; Poley, M.; Tzror, C.; Yaari, Z.; Krayem, M.; Kasten, S.; Nawy, G.; Herman, A.; Nir, Y.; Akrish, S.; Klein, T.; Shainsky-Roitman, J.; Hershkovitz, D.; Schroeder, A., Proteolytic Nanoparticles Replace a Surgical Blade by Controllably Remodeling the Oral Connective Tissue. *ACS Nano* **2018,** 12, 1482-1490.

35. Kieler-Ferguson, H. M.; Chan, D.; Sockolosky, J.; Finney, L.; Maxey, E.; Vogt, S.; Szoka, F. C., Encapsulation, Controlled Release, and Antitumor Efficacy of Cisplatin Delivered in Liposomes Composed of Sterol-Modified Phospholipids. *Eur. J. Pharm. Sci.* **2017,** *103*, 85-93.

36. Redondo-Morata, L.; Giannotti, M. I.; Sanz, F., Influence of Cholesterol on the Phase Transition of Lipid Bilayers: A Temperature-Controlled Force Spectroscopy Study. *Langmuir-* **2012,** *28*, 12851-12860.

37. Harper, C. R.; Jacobson, T. A., The Fats of Life: The Role of Omega-3 Fatty Acids in the Prevention of Coronary Heart Disease. *Arch. Intern. Med.* **2001,** *161*, 2185-2192.

38. Goldman, E.; Zinger, A.; da Silva, D.; Yaari, Z.; Kajal, A.; Vardi-Oknin, D.; Goldfeder, M.; Schroeder, J. E.; Shainsky-Roitman, J.; Hershkovitz, D., Nanoparticles Target Early-Stage Breast Cancer Metastasis *In Vivo*. *Nanotechnology* **2017,** *28*, 43LT01.

39. Klibanov, A. L.; Maruyama, K.; Torchilin, V. P.; Huang, L., Amphipathic Polyethyleneglycols Effectively Prolong the Circulation Time of Liposomes. *FEBS Lett.* **1990,** *268*, 235-237.

40. Dolor, A.; Szoka, F. C., Jr., Digesting a Path Forward: The Utility of Collagenase Tumor Treatment for Improved Drug Delivery. *Mol Pharmaceutics* **2018,** *15*, 2069-2083.

41. Delire, B.; Starkel, P.; Leclercq, I., Animal Models for Fibrotic Liver Diseases: What We Have, What We Need, and What Is under Development. *J. Clin. Transl. Hepatol.* **2015,** *3*, 53-66.

42. Liedtke, C.; Luedde, T.; Sauerbruch, T.; Scholten, D.; Streetz, K.; Tacke, F.; Tolba, R.; Trautwein, C.; Trebicka, J.; Weiskirchen, R., Experimental Liver Fibrosis Research: Update on Animal Models, Legal Issues and Translational Aspects. *Fibrog. Tissue Repair* **2013,** *6*, 19.

43. Yanguas, S. C.; Cogliati, B.; Willebrords, J.; Maes, M.; Colle, I.; van den Bossche, B.; de Oliveira, C.; Andraus, W.; Alves, V. A. F.; Leclercq, I.; Vinken, M., Experimental Models of Liver Fibrosis. *Arch. Toxicol.* **2016,** *90*, 1025-1048.

44. Jacobs, A.; Warda, A. S.; Verbeek, J.; Cassiman, D.; Spincemaille, P., An Overview of Mouse Models of Nonalcoholic Steatohepatitis: From Past to Present. *Curr. Protoc. Mouse Biol.* **2016,** *6*, 185-200.

45. He, Z.; Wan, X.; Schulz, A.; Bludau, H.; Dobrovolskaia, M. A.; Stern, S. T.; Montgomery, S. A.; Yuan, H.; Li, Z.; Alakhova, D. ; Sokolsky, M.; Darr, D. B.; Perou, C. M.; Jordan, R.; Luxenhofer, R.; Kabanov, A. V., A High Capacity Polymeric Micelle of Paclitaxel: Implication of High Dose Drug Therapy to Safety and *In Vivo* Anti-Cancer Activity. *Biomaterials* **2016,** *101*, 296-309.

46. Plaks, V.; Koopman, C. D.; Werb, Z., Cancer. Circulating Tumor Cells. *Science* **2013,** *341*, 1186-1188.

47. Velez, D. O.; Tsui, B.; Goshia, T.; Chute, C. L.; Han, A.; Carter, H.; Fraley, S. I., 3d Collagen Architecture Induces a Conserved Migratory and Transcriptional Response Linked to Vasculogenic Mimicry. *Nat. Commun.* **2017,** *8*, 1651.

48. Murty, S.; Gilliland, T.; Qiao, P.; Tabtieng, T.; Higbee, E.; Al Zaki, A.; Pure, E.; Tsourkas, A., Nanoparticles Functionalized with Collagenase Exhibit Improved Tumor Accumulation in a Murine Xenograft Model. *Part. Part. Syst. Charact.* **2014,** *31*, 1307-1312.

49. Goodman, T. T.; Olive, P. L.; Pun, S. H., Increased Nanoparticle Penetration in Collagenase-Treated Multicellular Spheroids. *Int. J. Nanomedi.* **2007,** *2* , 265-274.

50. Crist, D. W.; Sitzmann, J. V.; Cameron, J. L., Improved Hospital Morbidity, Mortality, and Survival after the Whipple Procedure. *Ann. Surg.* **1987,** *206*, 358.

51. Fong, Z. V.; Ferrone, C. R.; Lillemoe, K. D.; Fernandez-Del Castillo, C., Intraductal Papillary Mucinous Neoplasm of the Pancreas: Current State of the Art and Ongoing Controversies. *Ann. Surg.* **2016,** *263*, 908-917.

52. Bockhorn, M.; Uzunoglu, F. G.; Adham, M.; Imrie, C.; Milicevic, M.; Sandberg, A. A.; Asbun, H. J.; Bassi, C.; Buchler, M.; Charnley, R. M*,*; Conlon, K.; Cruz, L. F.; Dervenis, C.; Fingerhutt, A.; Friess, H.; Gouma, D. J.; Hartwig, W.; Lillemoe, K. D.; Montorsi, M*;* Neoptolemos, J. P., *et al.*, Borderline Resectable Pancreatic Cancer: A Consensus Statement by the International Study Group of Pancreatic Surgery (Isgps). *Surgery* **2014,** *155*, 977-988.

53. Burris 3rd, H.; Moore, M. J.; Andersen, J.; Green, M. R.; Rothenberg, M. L.; Modiano, M. R.; Cripps, M. C.; Portenoy, R. K.; Storniolo, A. M.; Tarassoff, P., Improvements in Survival and Clinical Benefit with Gemcitabine as First-Line Therapy for Patients with Advanced Pancreas Cancer: A Randomized Trial. *J. Clin. Oncol.* **1997,** *15*, 2403-2413.

54. Parker, S. L.; Tong, T.; Bolden, S.; Wingo, P. A., Cancer Statistics, 1996. *CA- Cancer J. Clin.* **1996,** *46*, 5-27.

55. Iredale, J. P.; Thompson, A.; Henderson, N. C., Extracellular Matrix Degradation in Liver Fibrosis: Biochemistry and Regulation. *Biochim. Biophys. Acta.* **2013,** *1832*, 876-883.

56. Badalamente, M. A.; Hurst, L. C.; Hentz, V. R., Collagen as a Clinical Target: Nonoperative Treatment of Dupuytren's Disease. *J. Hand. Surg. Am.* **2002,** *27*, 788-798.

57. Bayat, A.; McGrouther, D. A., Management of Dupuytren's Disease – Clear Advice for an Elusive Condition. *Ann. R. Coll. Surg. Engl.* **2006,** *88*, 3-8.

58. Holmbeck, K.; Bianco, P.; Caterina, J.; Yamada, S.; Kromer, M.; Kuznetsov, S. A.; Mankani, M.; Gehron Robey, P.; Poole, A. R.; Pidoux, I. Ward, J. M.; Birkedal-Hansen, H., Mt1-Mmp-Deficient Mice

Develop Dwarfism, Osteopenia, Arthritis, and Connective Tissue Disease Due to Inadequate Collagen Turnover. *Cell* **1999,** *99*, 81-92.

59. Goel, A.; Shrivastava, P., Post-Burn Scars and Scar Contractures. *Indian J. Plast. Surg.* **2010,** *43*, S63-S71.

60. Hingorani, S. R.; Wang, L.; Multani, A. S.; Combs, C.; Deramaudt, T. B.; Hruban, R. H.; Rustgi, A. K.; Chang, S.; Tuveson, D. A., Trp53r172h and Krasg12d Cooperate to Promote Chromosomal Instability and Widely Metastatic Pancreatic Ductal Adenocarcinoma in Mice. *Cancer Cell* **2005,** *7*, 469-483.

61. Torres, M. P.; Rachagani, S.; Souchek, J. J.; Mallya, K.; Johansson, S. L.; Batra, S. K., Novel Pancreatic Cancer Cell Lines Derived from Genetically Engineered Mouse Models of Spontaneous Pancreatic Adenocarcinoma: Applications in Diagnosis and Therapy. *PloS One* **2013,** *8*, e80580.

62. Herreros-Villanueva, M.; Hijona, E.; Cosme, A.; Bujanda, L., Mouse Models of Pancreatic Cancer. *World J. Gastroenterol.* **2012,** *18*, 1286.

63. Qiu, W.; Su, G. H., Development of Orthotopic Pancreatic Tumor Mouse Models. *Methods Mol. Biol.* **2013,** *980*, 215-223.

64. Johnson, T. D.; Braden, R. L.; Christman, K. L., Injectable ECM Scaffolds for Cardiac Repair. *Methods Mol. Biol.* **2014**,109-120.

65. Lübtow, M. M.; Hahn, L.; Haider, M. S.; Luxenhofer, R., Drug Specificity, Synergy and Antagonism in Ultrahigh Capacity Poly(2-Oxazoline)/Poly(2-Oxazine) Based Formulations. *J. Am. Chem. Soc.* **2017,** *139*, 10980-10983.